PART 1. Supplementary method :

Crossover correction for scalar and vector magnetic anomalies

Authors: Hanjin Choe, Jérôme Dyment

Affiliations: Université de Paris, Institut de physique du globe de Paris, CNRS, 75005 Paris, France

Reliable marine magnetic data are generally acquired by deploying a proton precession magnetometer (PPM), which provides absolute measurements of the field vector intensity that can be immediately used after removing a core field model. To try to access the three components of the field vector and, in some cases, to avoid the deployment of a PPM, shipboard three-component magnetometers (STCM) have been installed on research vessels, mostly in Japan. As a result, large amounts of STCM data are available around the Japan Trench and cover areas where PPM surveys have not been conducted so far (Fig. S1). However, STCM data requires some heavier processing to remove the ship magnetic effect and recover the magnetic field in proper geographical coordinates (Isezaki, 1986). Despite correction of the induced and remanent magnetization of the ship, other magnetic effects remain that prevent merging the magnetic anomalies obtained from STCM data, which are only relative, together or with those derived from the absolute PPM data (Fig. S2A and B).

We built our magnetic map of the Japan Trench by first considering the absolute PPM data, then including the relative total field computed from the STCM data. The PPM data gathered from different cruises and databases are leveled (for instance using X2SYS, a crossover analytic tool available in GMT; Wessel, 2010). In the next step, the corrected PPM data are used as a reference to tie the STCM surveys at their intersections. To do so, we first attempt to apply a constant leveling to individual cruise, but erroneous linear trends remain along STCM tracks (Fig. S2C). These errors may result from the accumulation of viscous magnetization by the ferromagnetic ship body as the ship keeps the same heading. This effect is not taken into account by Isezaki (1986). Viscous magnetization is difficult to estimate for a cruise with changing headings. To approximate its effect by a linear trend, we split the STCM survey tracks in straight segment lines.

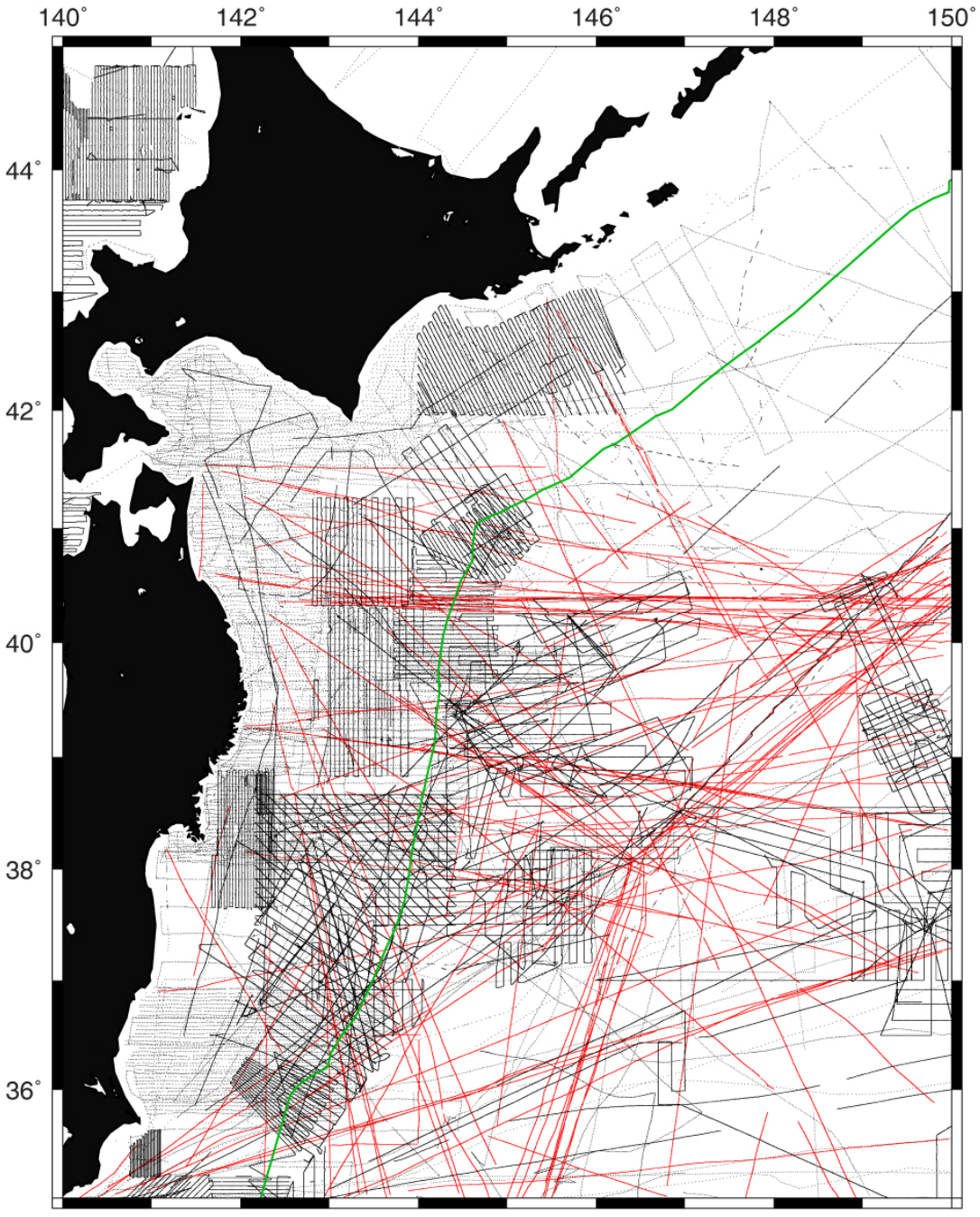

Figure S1. Marine magnetic surveys NE of Japan. Red solid lines display the STCM survey tracks, black solid lines the PPM survey tracks. The green solid line shows the Japan and Kuril trenches.

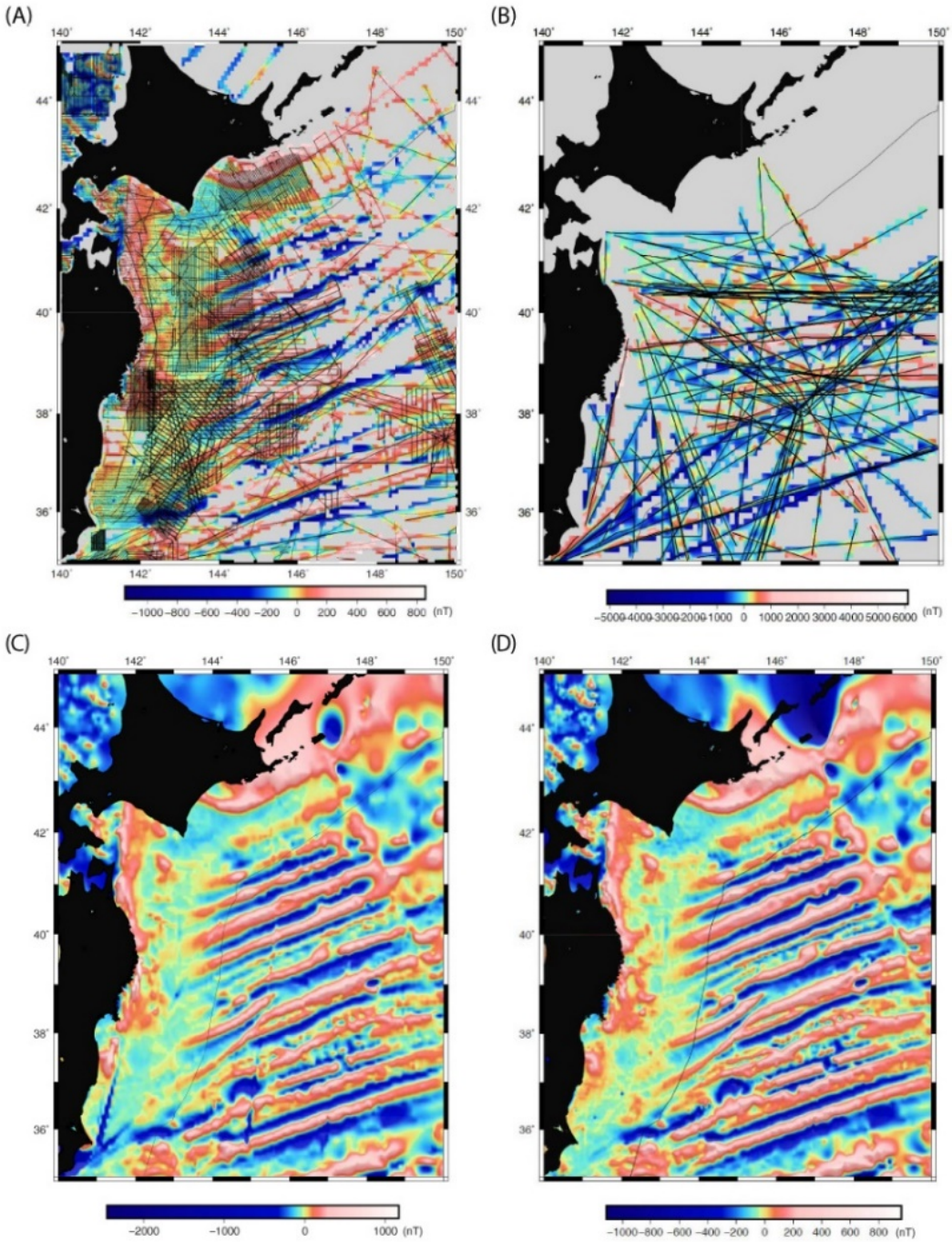

Figure S2. (A) Magnetic anomaly grid from the leveled PPM data; (B) Magnetic anomaly grid from the corrected STCM data; (C) Magnetic anomaly grid after leveling the corrected STCM data to adjust them to the leveled PPM data; (D) Magnetic anomaly grid after leveling and de-trending the corrected STCM data to adjust them to the leveled PPM data.

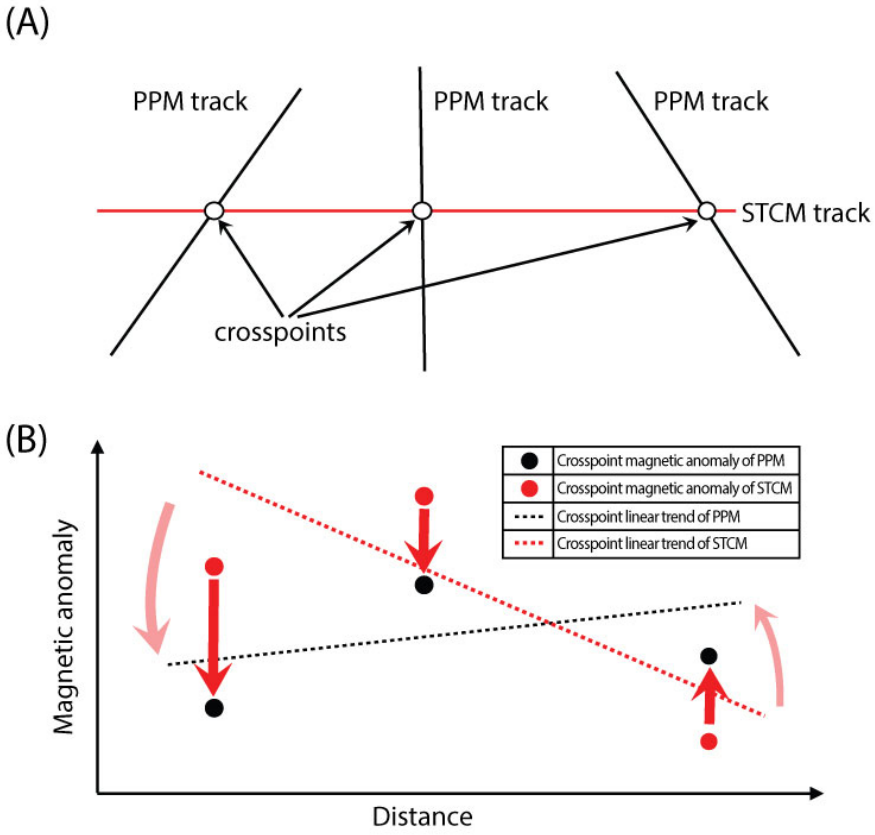

Figure S3. Schematic explanation of crossover method. The method is applied to de-trend the STCM data to adjust them to the PPM data.

We apply a linear regression method at crossover points between the considered STCM segment and the PPM data. We determine the crossover points and average separately the PPM and STCM values for each crossover point within 1 arc-minute radius. If only one crossover point exists or if there are only two and the distance between them is less than 20 km, we discard the STCM segment. We compute separate linear trends from the PPM and STCM values at the crossover points of the segment to evaluate the residual trend, i.e. the difference between the linear trends from STCM values at crossover points and from PPM values at the same points and remove it from the STCM data (Fig. S3). This method properly eliminates the misfit between the STCM and PPM data, as shown by an example with real data (Fig. S4).

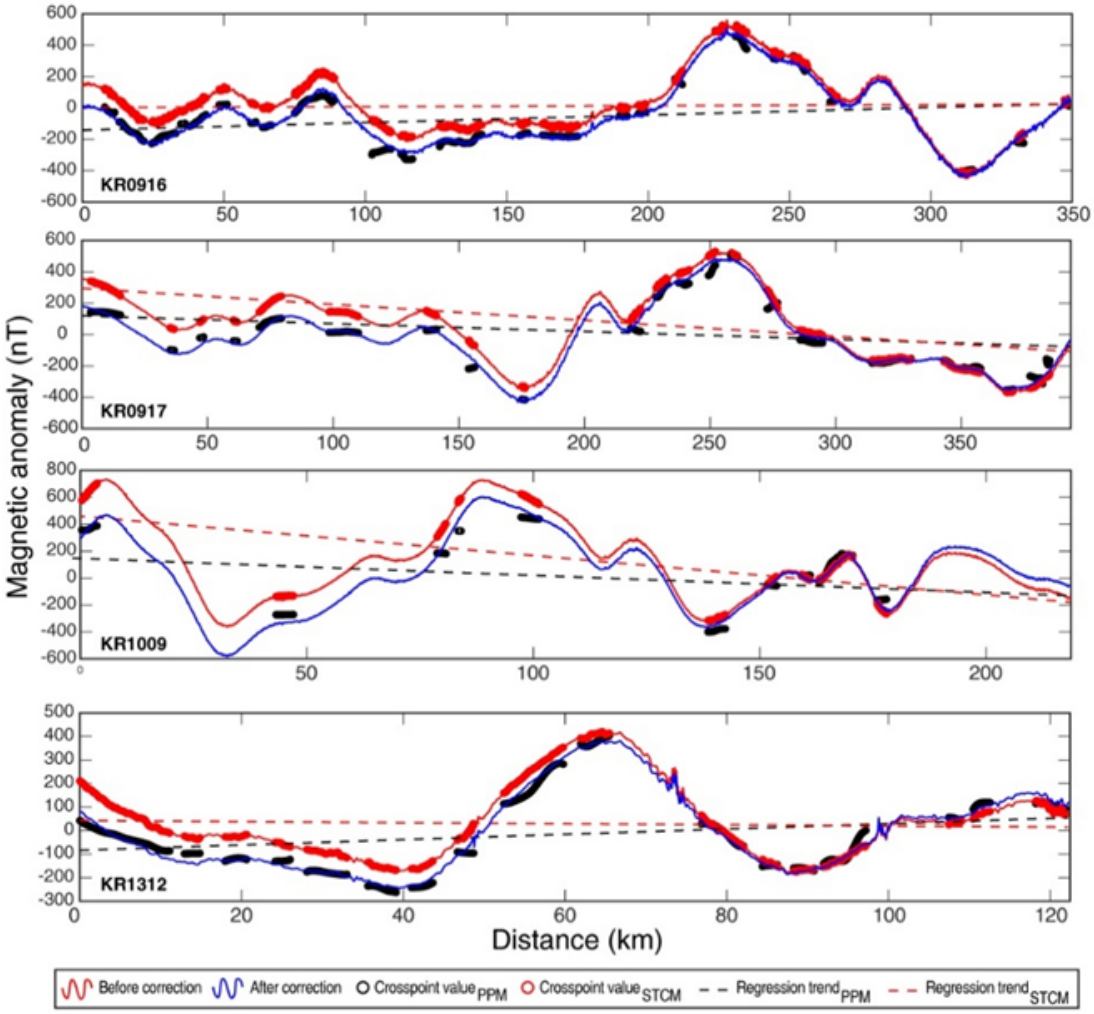

Figure S4. Method to de-trend the STCM data to adjust them to the PPM data applied to real data. Red solid line, STCM data affected by the ship viscous magnetization approximated by a linear trend; Red circles, STCM at crossover points; Red dashed line, linear regression of STCM at crossover points; Black circles, PPM at crossover points; Black dashed line, linear regression of PPM at crossover points; Blue solid line, corrected STCM data after removing the linear trend from STCM at crossover points and adding the linear trend on PPM at crossover points.

The histogram of the misfits shows the significant improvement obtained by de-trending the STCM data along straight segments compared to the simple leveling of the STCM data cruise by cruise and to the initial data (Fig. S5). The standard deviation (1σ) is 104.9 nT, 68.9 nT and 49.2 nT for the original data, the leveled data using the conventional crossover analysis method, and our crossover algorithm including de-trending of the data.

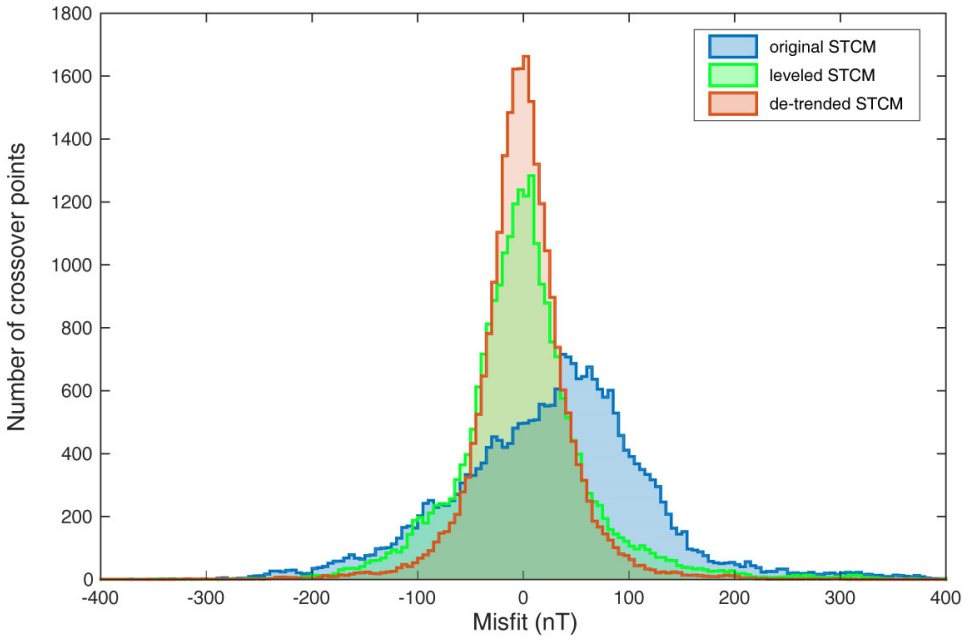

Figure S5. Histogram of the misfits between leveled PPM data and various sets of STCM data. Blue, initial STCM data; Green, STCM data leveled cruise by cruise; Red, STCM data de-trended along straight segments.

We analyze the relationship of the residual trends obtained from R/V Kairei and R/V Mirai with the ship heading (Fig. S6). Despite significant scatter, the residual trend shows a symmetrical distribution that can be approximated by a sine function of the ship heading. Although this is verified for datasets from both R/V Kairei and R/V Mirai, the residual trends for these two ships show opposite signs.

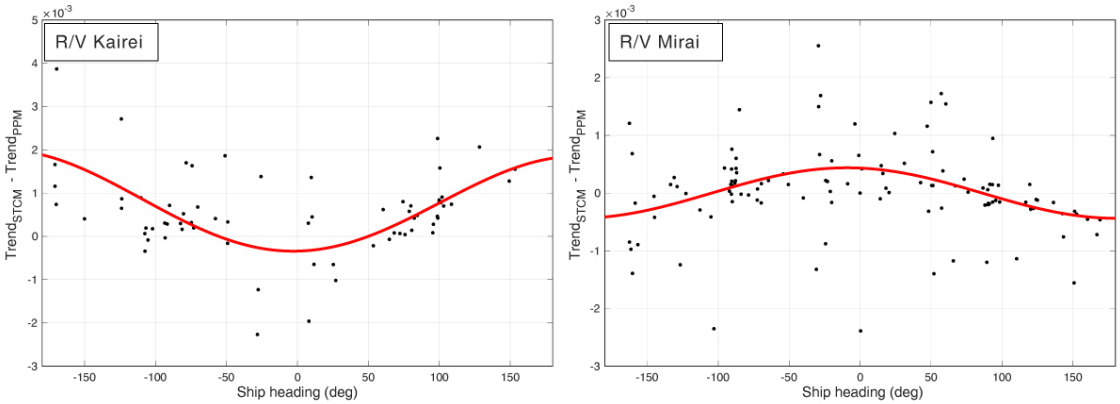

Figure S6. Relationship of the residual trend with the ship heading. Black dots, data from R/V Kairei (left) and R/V Mirai (right). Red solid lines, best fitting Sine functions.

To understand these observations, let consider the ship as a big magnet (Fig. S7). In mid-latitudes, such a magnet produces a dipolar anomaly with a positive lobe toward the Equator and a negative lobe toward the pole (see Dyment and Arkani-Hamed, 1998; Fig. 1B, for examples). We can therefore suspect that the STCM is located forward on R/V Kairei (resp. backward on R/V Mirai) to sample the negative (resp. positive) lobe when the ship is heading North. When the ship is heading in different directions, the STCM is sampling different parts of the ship magnetic anomaly. Instead of the anomaly - as it would be in a very similar way if we were discussing the effect of induced magnetization, Figure S6 and S7 are considering the linear trend of the anomaly created by viscous magnetization. These figures offer a way to model and possibly correct the ship viscous magnetization in future surveys.

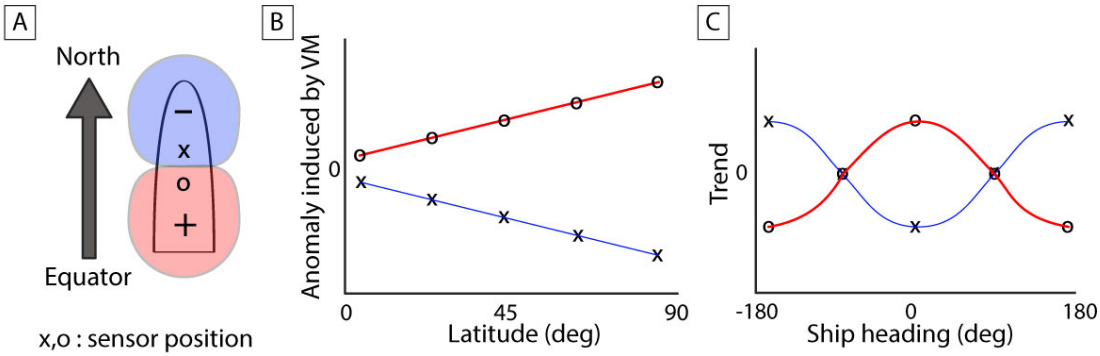

Figure S7. (A) Schematic illustration of the magnetic anomaly of a ferromagnetic ship body when the ship is heading to the north at northern mid-latitudes. "X" and "O" signs mark the location of the STCM sensor on R/V Kairei and R/V Mirai, respectively. (B) Expected magnetic field variations trlated to the acquisition of viscous magnetization, following Fig. S7A. (C) Predicted relationship of the residual trend with the ship heading for R/V Kairei (blue) and R/V Mirai (red).

REFERENCES CITED

Isezaki, N., 1986, A new shipboard three-component magnetometer: GEOPHYSICS, v. 51, p. 1992–1998, doi:10.1190/1.1442054.

Dyment, J., and Arkani-Hamed, J., 1998, Contribution of lithospheric remanent magnetization to satellite magnetic anomalies over the world's oceans: Journal of Geophysical Research: Solid Earth, v. 103, p. 15423–15441, doi:10.1029/97JB03574.

Wessel, P., 2010, Tools for analyzing intersecting tracks: The x2sys package: Computers & Geosciences, v. 36, p. 348–354, doi:10.1016/j.cageo.2009.05.009.

PART 2. Supplementary discussion:

Uncertainties in the slab geometry

Authors: Hanjin Choe, Jérôme Dyment

Affiliations: Université de Paris, Institut de physique du globe de Paris, CNRS, 75005 Paris, France

Currently, two open-source slab grids, Slab1.0 (Hayes et al., 2012) and Slab2 (Hayes et al., 2018), are widely used for various geophysical analysis. A careful analysis of Fig. 3A (see main text) reveals that the maximum gradient of the remaining amounts of magnetization (RAM) is not observed at the exact same depths for the five investigated magnetic anomalies. These small discrepancies may result from uncertainties in the slab geometry. In order to choose the best slab geometry grid, we compared the two grids to recently published seismic sections in the study area (Kodaira et al., 2017) and observed a good coincidence between the seismic sections and Slab1.0, and significant discrepancies reaching 4 km with Slab2 (Fig. S8).

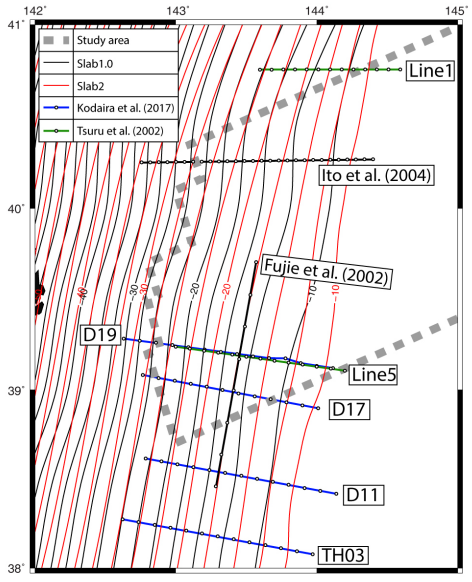

Figure S8. Comparison between the two slab grids and published seismic profiles. Black solid lines indicate the grid contour of Slab1.0 (Hayes et al., 2012); Red solid lines indicate the grid contour of Slab2 (Hayes et al., 2018). The interval of grid contour depths is 2.5 km. Blue solid lines with black circles indicate active seismic lines of Kodaira et al. (2017). Green solid lines with black circles indicate active seismic lines of Tsuru et al. (2002). Black solid lines with black circles indicate survey tracks used in Fujie et al. (2002) and Ito et al. (2004).

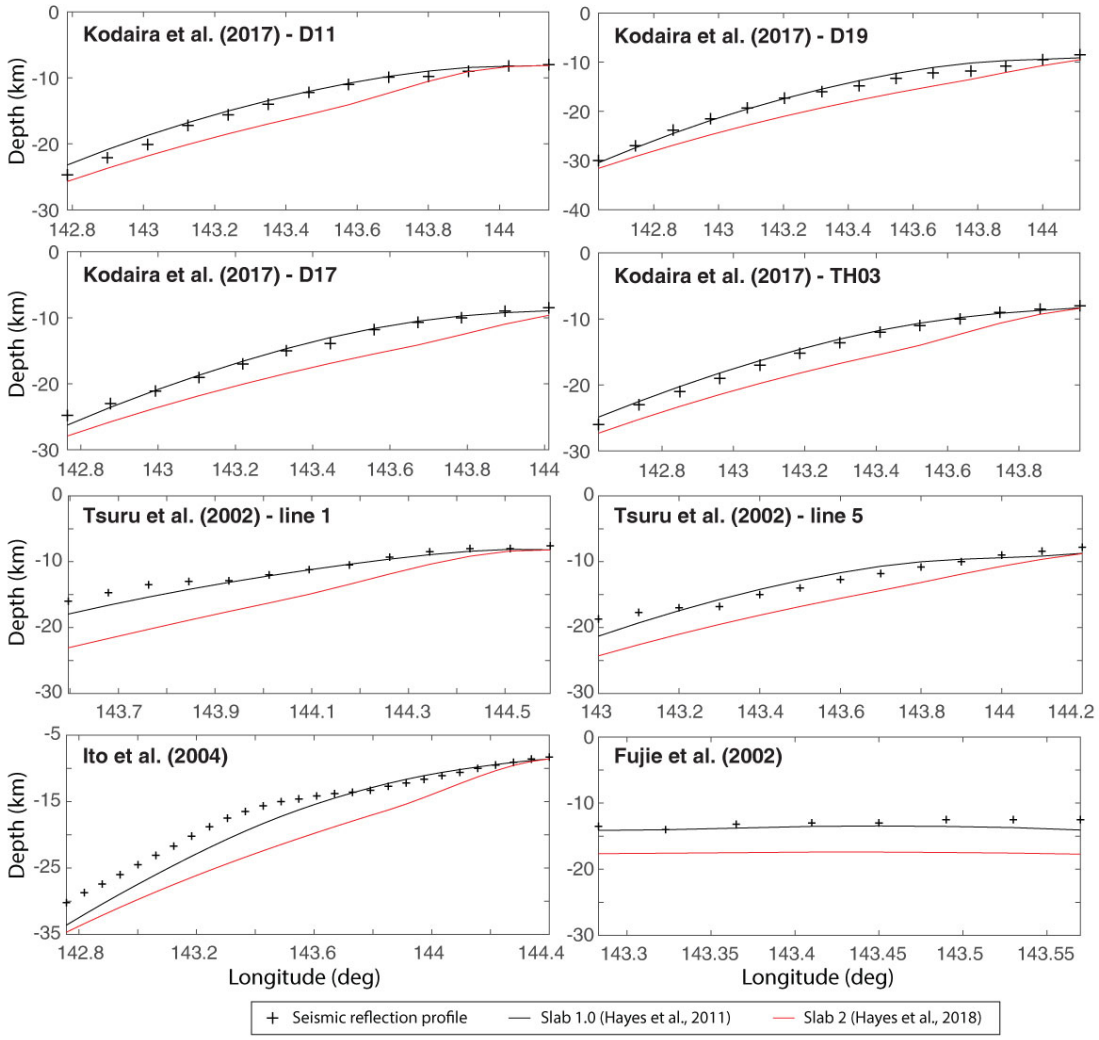

Figure S9. Comparison between slab geometry from seismic data (black crosses) and the two Slab grids along each seismic line (black solid line from Slab1.0, red solid line from Slab2). Slab1.0 agrees well with the seismic profiles whereas Slab2 is systematically deeper.

Fig. S9 shows the slab depth along the four seismic lines. Comparison between depths from the seismic profiles and the two slab grids shows unambiguously that Slab1.0 has much smaller misfits (usually less than ± 2 km) than Slab2, which predicts generally a deeper slab and larger misfits (2 to 5 km). We suspect that the degraded slab geometry in Slab2 results from improper digitization of Figure 1B of Kodaira et al. (2017), which extends in longitude from 142°E to 144.75°E. This fractional eastern bound may have misled the digitizer. We therefore decided to use Slab1.0 in our analysis.

REFERENCES CITED

Fujie, G., Kasahara, J., Hino, R., Sato, T., Shinohara, M., and Suyehiro, K., 2002, A significant relation between seismic activities and reflection intensities in the Japan Trench region: Geophysical Research Letters, v. 29, p. 4–7, doi:10.1029/2001GL013764.

Hayes, G.P., Wald, D.J., and Johnson, R.L., 2012, Slab1.0: A three-dimensional model of global subduction zone geometries: Journal of Geophysical Research: Solid Earth, v. 117, doi:10.1029/2011JB008524.

Hayes, G.P., Moore, G.L., Portner, D.E., Hearne, M., Flamme, H., Furtney, M., and Smoczyk, G.M., 2018, Slab2, a comprehensive subduction zone geometry model: Science, v. 362, p. 58–61, doi:10.1126/science.aat4723.

Ito, A., Fujie, G., Tsuru, T., Kodaira, S., Nakanishi, A., and Kaneda, Y., 2004, Fault plane geometry in the source region of the 1994 Sanriku-oki earthquake: Earth and Planetary Science Letters, v. 223, p. 163–175, doi:10.1016/j.epsl.2004.04.007.

Kodaira, S., Nakamura, Y., Yamamoto, Y., Obana, K., Fujie, G., No, T., Kaiho, Y., Sato, T., and Miura, S., 2017, Depth-varying structural characters in the rupture zone of the 2011 Tohoku-oki earthquake: Geosphere, v. 13, p. 1408–1424, doi:10.1130/GES01489.1.

Tsuru, T., Park, J.-O., Miura, S., Kodaira, S., Kido, Y., and Hayashi, T., 2002, Along-arc structural variation of the plate boundary at the Japan Trench margin: Implication of interplate coupling: Journal of Geophysical Research: Solid Earth, v. 107, p. ESE 11-1-ESE 11-15, doi:10.1029/2001JB001664.

PART 3. Supplementary discussion:

Effect of a dipping slab on the inclination and declination of magnetization, consequences on the amplitude of magnetic anomalies

Authors: Hanjin Choe, Jérôme Dyment

Affiliations: Université de Paris, Institut de physique du globe de Paris, CNRS, 75005 Paris, France

The slope of the subducting oceanic lithosphere gradually increases with depth. This increasing slope causes a progressive change in the direction of the remanent magnetization vector. Slight changes in this direction may generate significant effect on the synthetic magnetic anomalies, affecting the determination of the Remaining Amount of Magnetization (RAM; see Data and Methods section). In this appendix, we examine this effect for the Japan Trench area and compare the amplitude of modeled anomalies considering, or not, the tilt induced by the slab geometry.

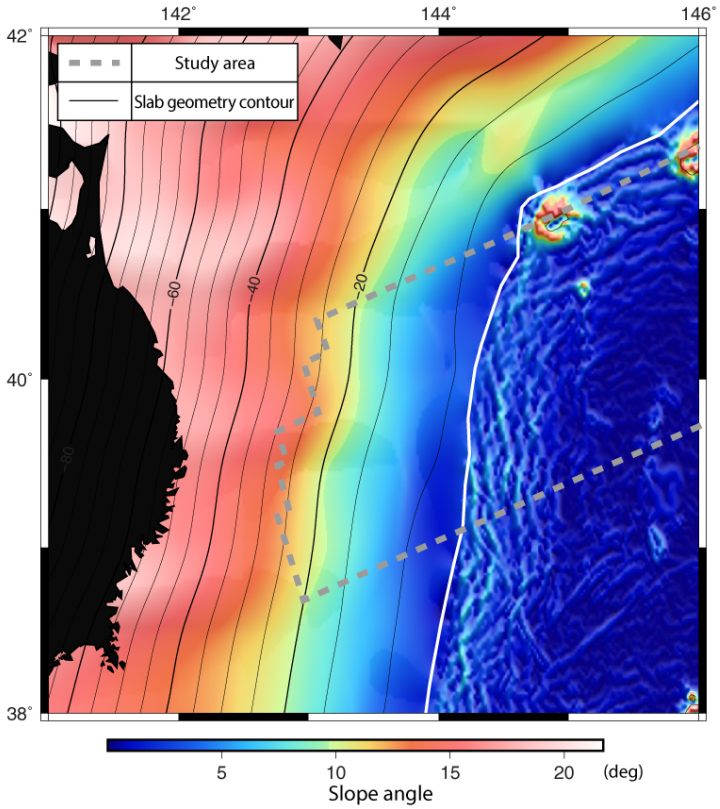

Figure S10. Tilt angle grid of subducting oceanic crust based on Slab1.0. Gray dashed line indicates study area in the main text. Black solid lines indicate the grid contour of Slab1.0 (Hayes et al., 2012). The interval of grid contour depths is 5 km. White solid line describes the location of Japan Trench.

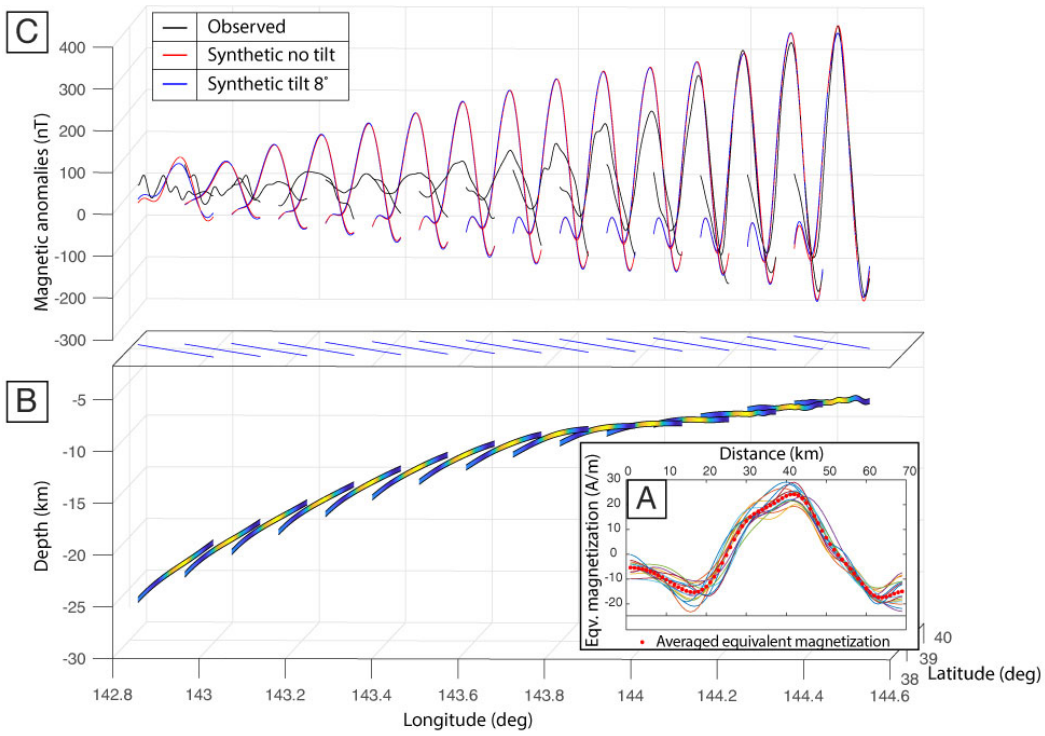

Figure S11. **A:** Equivalent magnetization inverted from profiles across magnetic anomaly M10n before subduction (location: see Fig. 1C, orange box). Red dotted curve indicates the average equivalent magnetization adopted for further modeling. **B:** Three-dimensional view of the source layer and magnetization intensity (color) used to model the synthetic magnetic anomalies. Blue solid lines on top indicate location of the profiles. **C**: Three-dimensional view of the observed (black), synthetic magnetic anomalies with no tilt (red) and with a tilt of 8° (blue) across magnetic anomaly M10n after subduction.

The slope of the source geometry, shown in Figure S10, increase from a bit less than 3° west of the Japan Trench to 10° at 20 km bsl, where the seafloor spreading magnetic anomaly disappear. To check the effect of tilting the magnetization vector beneath 12km bsl, we used a 82° inclination and 103° azimuth (respectively a 90° inclination) to forward-model reduced-to-the-pole magnetic anomalies taking the tilt into account (respectively not taking the tilt into account). We compared the difference of these synthetic anomalies (Fig. S11) and the difference of the RAM deduced from these anomalies (Fig. S12). These differences are negligible and do not affect the result of our study.

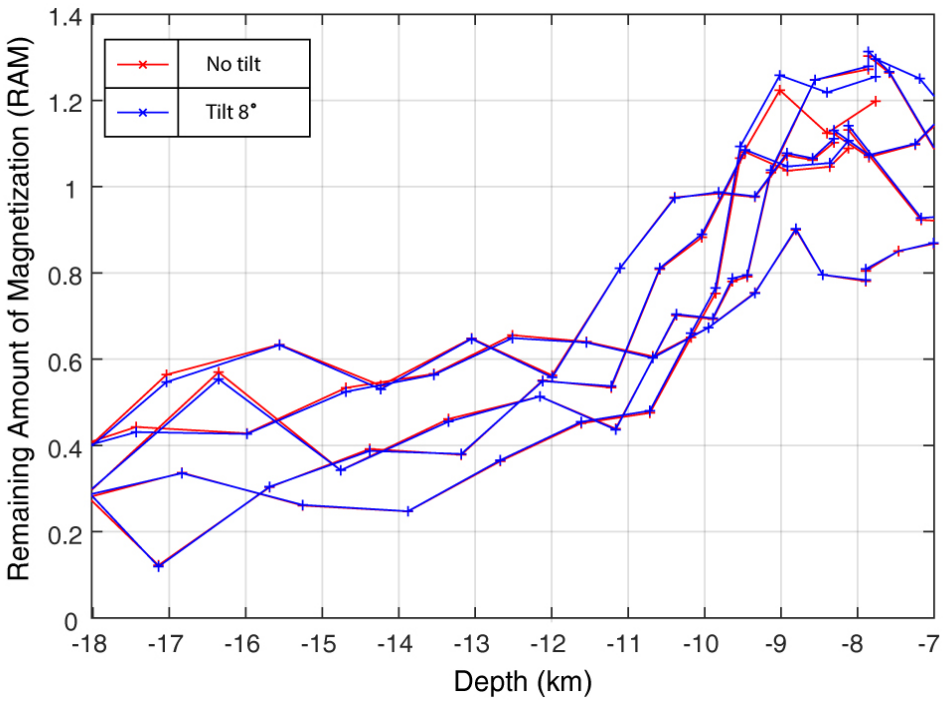

Figure S12. Remaining Amount of Magnetization (RAM) versus depth of subducting slab surface. Blue (respectively red) crosses and solid lines indicate the RAM considering (respectively not considering) the tilt of the remanent magnetization vector. The result shows no significant change in RAM values.